THE SUBSTRUCTURE ISOLATION METHOD FOR LOCAL ANALYSIS AT THE SUBSTRUCTURAL LEVEL

Jilin Hou[*], **Łukasz Jankowski**[†], **Jinping Ou**[‡]

[*,‡] Dalian University of Technology
School of Civil Engineering
Linggong Road, 2
116024, Ganjingzi District, Dalian City, Liaoning Province, China
e-mail: hou.jilin@hotmail.com, oujinping@dlut.edu.cn, web page: http://sche.dlut.edu.cn

[†] Institute of Fundamental Technological Research (IPPT PAN)
Department of Intelligent Technologies
ul. Pawińskiego, 5b
02-106, Warsaw, Poland
e-mail: ljank@ippt.gov.pl, web page: http://smart.ippt.gov.pl

[*] Corresponding author

Key words: Substructuring, Structural Health Monitoring, SHM, Damage identification, Local analysis.

Summary. *This paper presents the substructure isolation method, which a novel method for substructural analysis and structural health monitoring (SHM) at the local level. The motivation behind it are the facts that global SHM of large and complex structures is generally difficult and that often only small substructures are crucial and require monitoring. These facts suggest that there is a need for ways of applying global SHM approaches locally, which is impossible with typical substructuring methods. The paper offers an overview of the common substructuring approaches and describes the substructure isolation method. The method splits the task of local monitoring into two stages: (1) Isolation; the outside influences are numerically eliminated from the measured response of the substructure. (2) Local SHM; all methods aimed originally at global SHM can be used with the constructed response of the isolated substructure. Local analysis is possible in time domain as well as in frequency domain; in offline and in online time regimes. The method is illustrated in a numerical example and substantiated in an experimental study using a damaged cantilever beam; the robustness of the isolation with respect to unknown modifications of the outside structure is tested.*

1. INTRODUCTION

Research on damage identification in SHM often focus on large specialized structures, such as bridges, tall buildings, dams, etc. Such complex structures are difficult to be monitored globally using approaches of low frequency SHM due to several reasons:

1. *Accuracy and reliability of parametric numerical models.* Boundary conditions and non-linear components are often hard to model or determine, which might be reflected in a poor accuracy of any global parametric numerical model of the monitored structure.

2. *Poor numerical convergence.* In large problems of global identification or model updating the numerical convergence is usually undermined by a large number of independent unknown parameters that need to be identified simultaneously. This results in significant ill-conditioning.

3. *Large number of sensors* that are necessary to guarantee uniqueness of the result of a global identification. The reasons are the large number of involved unknowns and the local-only sensitivity of the global response with respect to local damages. This is costly and rarely feasible in practice.

4. *Unknown excitations.* Response of the global structure is often influenced by many excitations that cannot be measured and often even characterized accurately enough.

As a result, in monitoring of large and complex structures, data-driven (pattern-recognition) approaches have often to be used at the expense of accuracy and physicality of model-based SHM. However, in many practical applications only small local substructures are crucial and need monitoring, which suggests that model-based SHM approaches could be applied locally. Such small substructures feature much fewer structural parameters and unknown factors that need to be identified and controlled, which makes local modeling and analysis much more feasible in comparison to global approaches.

1.1 State-of-the-art

The body of research on damage detection through localized analysis is relatively large. To detect local damage, one can compare locally sensitive information, such as local strain or local modal characteristics, extracted from the dynamic structural responses measured before and after the damage occurs. However, a substructure is a local part of the global structure, and so it is not independent of the global structure. In order to focus on the substructure only, most of the existing approaches separate the substructure from the global structure by partitioning the global equation of motion. The generalized interface forces are then used for coupling both structures and so they need to be identified together with substructural parameters. The local identification is performed usually in a model-based manner and requires a general parametric numerical model of the substructure to be known beforehand.

The substructural approach has been probably first considered by Koh et al. [2] in the context of structural identification and called a substructural identification (SSI) or a divide-and-conquer strategy. This method applies the extended Kalman filter with weighted global iteration to substructures with and without overlapping members; in [3], it is developed into a progressive structural identification approach, which identifies the global structure through identification of progressively growing substructures. In [4], Yun and Lee employ an ARMAX model of the substructure and a sequential prediction error method to locally estimate unknown parameters that are related to damages; complete measurement of the substructure is necessary, including the interior excitations and the response in all its DOFs. Tee et al. [5] apply the substructural strategy in the field of SHM and propose two methods aimed at first- and second-order model identification and damage assessment at the substructural level. The methods are based on the eigensystem realization algorithm (ERA) and the observer/Kalman filter; in [6], they are combined with a model condensation approach, which allows the number of necessary measurements to be reduced. In all these and similar methods, complete measurement of interface response is necessary: the measured response is treated as a known input to the substructure. A method that does not require the interface responses to be measured directly is proposed by Koh et al. in [1], where the generalized interface forces between the substructure and the global structure are identified simultaneously with the unknown physical parameters of the substructure using local frequency response functions. Different sets of internal response measurements are used to obtain different estimates of the interface forces; the identification procedure amounts to minimization of the discrepancy between them. Yang and Huang propose in [7] a sequential nonlinear least-square method to estimate unknown excitations, physical parameters of the substructure as well as the interface forces. Lei et al. propose in [8] a related algorithm for identification of non-linear substructural parameters; the algorithm is based on the sequential application of the extended Kalman estimator for the non-linear structural parameters and the least-squares indirect estimation of the unmeasured interface forces. Both methods require only a limited number of output measurements, and they can trace damages changing with time. A method based on multi-feature genetic algorithm was used by Trinh and Koh [9] to estimate substructural mass, damping and stiffness parameters. Xing and Mita [10] confine each substructure of a multi-storey shear building to a few DOFs only and use overlapping substructures; they apply directly the ARMAX method for local identification. Wang et al. [11] employ the concept of the quasi-static displacement vector to simplify the generalized interface forces, and use a method based on a genetic algorithm to identify the substructure.

1.2 Separation vs. isolation of substructures

All the methods mentioned above can be collectively called *substructure separation* methods, since they rather separate than isolate the substructure from the global structure: although separated, the substructure and the global structure remain coupled to each other via the unknown interface forces. Consequently, all the discussed identification procedures need to account for the unknown interface forces besides the unknown substructural parameters. However, forces and structural parameters are variables of very different characteristics, and thus all these

identification methods, although effective, are not standard and have to be specifically tailored to be used at the substructural level. As a result,

- Standard and widely-researched model updating or health monitoring methods cannot be directly applied to the separated substructure.

- Many substructuring methods appear to be limited to small substructures that have simple interfaces. A simple shear building is such a structural model and it is widely used in most of the references mentioned above. However, in real applications structures are more complex, and their substructures have more DOFs and more complex interfaces.

To overcome these drawbacks, a *substructure isolation* method has been proposed [12–18]. The core idea of the isolation method is different: instead of separating the substructure and then identifying its parameters together with the unknown interface forces, the method splits the task of local identification into two conceptually distinct stages that are performed separately:

1. *Isolation of the substructure.* In this stage, the method numerically eliminates the outside influences of the global structure from the measured response of the substructure. The response constructed this way is the response of the substructure *as if* it was *physically isolated* from the global structure with supports placed on the interface. The process is equivalent to constructing an *isolated substructure*, which is an independent virtual structure with the same parameters as the real substructure, but isolated from the global structure with virtual supports placed on the interface.

2. *Local analysis and identification* of the isolated substructure. Any of the existing, well-researched methods aimed originally at global SHM can be used together with the computed response of the isolated substructure.

Such an approach places the substructure isolation method in a broader landscape of methods that use structural modifications, either physical or virtual, to increase the response sensitivity to selected structural parameters, see [19–22]. Notice that there are no unknown interface forces to be accounted for in the second stage. Moreover, response of the isolated substructure is constructed directly using measured responses of the substructure, so that no parametric numerical model is required at the isolation stage.

2. VIRTUAL SUPPORTS

The isolation method can be based on the notion of a virtual support [15] and introduced using the methodology of the virtual distortion method (VDM, [23]). The core idea of the VDM is to model the effects of local structural modifications using the equivalent pseudo loads and/or virtual distortions. Here, the same idea is used to model a *virtual fixed support*. It is modeled with the equivalent pseudo load that equals the generalized support reaction force that would occur, if the structure was physically supported. The time history of such an equivalent pseudo load can be computed using the natural condition that the modeled responses in all DOFs with virtual fixed supports vanish.

2.1 Naming convention

The response of the virtually supported structure to an external excitation $\mathbf{f}(t)$ is computed using several responses of the original unmodified structure. These responses are generated experimentally using two different types of excitations and measured using two types of sensors. The considered excitations can be divided into: (1) *Constraining excitations*, which are applied in all DOFs intended for virtual supports, and (2) *Basic excitation*, which is the external excitation $\mathbf{f}(t)$. The responses to these excitations are measured by the two following types of sensors: (1) *Constraining sensors*, which are linear sensors (displacement, velocity or acceleration) that need to be placed in all the DOFs intended for virtual supports, and (2) *Basic sensors*, which are linear sensors of any type placed in the structure in order to measure its response. The aim is to compute the response to the basic excitation that would be measured by the basic sensors, if the structure was physically supported in the considered DOFs. The excitations (basic and constraining) need not be measured for the purpose of the analysis.

Since there are two types of excitations and two types of sensors, four different types of response are measured altogether, see Table 1. Notice that $\mathbf{u}^{\mathrm{L}}(t)$ and $\mathbf{a}^{\mathrm{L}}(t)$ are vectors, while $\mathbf{B}^{\mathrm{up}}(t)$ and $\mathbf{B}^{\mathrm{ap}}(t)$ are matrices.

2.2 Virtual fixed supports

Assume that the original unmodified structure is subjected to an external excitation $\mathbf{f}(t)$ (basic excitation) and that the responses listed in Table 1 are measured and available. Virtual fixed supports are modeled with a pseudo load vector $\mathbf{p}^{0}(t)$, which acts in all the to-be-supported DOFs and which would equal the generalized support reaction forces, if the structure was physically supported. The structure is assumed to be linear, hence, with zero initial conditions, the modeled responses of the virtually supported structure can be expressed as follows:

$$\mathbf{a}(t) = \mathbf{a}^{\mathrm{L}}(t) + \int_{0}^{t} \mathbf{B}^{\mathrm{ap}}(t - \tau)\mathbf{p}^{0}(\tau)\,\mathrm{d}\tau, \tag{1a}$$

$$\mathbf{u}(t) = \mathbf{u}^{\mathrm{L}}(t) + \int_{0}^{t} \mathbf{B}^{\mathrm{up}}(t - \tau)\mathbf{p}^{0}(\tau)\,\mathrm{d}\tau, \tag{1b}$$

where the vectors $\mathbf{a}(t)$ and $\mathbf{u}(t)$ denote the responses of the constraining and basic sensors respectively. For the moment, the constraining excitations are assumed to be impulsive, so that

Table 1. Naming convention

	basic excitation $\mathbf{f}(t)$	constraining excitations*
basic sensors	$\mathbf{u}^{\mathrm{L}}(t)$	$\mathbf{B}^{\mathrm{up}}(t)$
constraining sensors*	$\mathbf{a}^{\mathrm{L}}(t)$	$\mathbf{B}^{\mathrm{ap}}(t)$

*Applied/placed in all the to-be-supported DOFs.

the matrices $\mathbf{B}^{\mathrm{up}}(t)$ and $\mathbf{B}^{\mathrm{ap}}(t)$ contain structural impulse response functions. Stated in the operator notation, Equations 1 take the following form of two large linear systems:

$$\mathbf{a}(t) = \mathbf{a}^{\mathrm{L}}(t) + \left(\boldsymbol{\mathcal{B}}^{\mathrm{ap}}\mathbf{p}^0\right)(t), \tag{2a}$$

$$\mathbf{u}(t) = \mathbf{u}^{\mathrm{L}}(t) + \left(\boldsymbol{\mathcal{B}}^{\mathrm{up}}\mathbf{p}^0\right)(t), \tag{2b}$$

where $\boldsymbol{\mathcal{B}}^{\mathrm{ap}}$ and $\boldsymbol{\mathcal{B}}^{\mathrm{up}}$ are the respective matrix convolution operators.

If the pseudo load vector $\mathbf{p}^0(t)$ is assigned such a value that it properly models the effects of fixed supports in the selected DOFs, then the responses of the constraining sensors to the basic excitation must vanish, as they are measured in the supported DOFs. In other words, $\mathbf{a}(t) = \mathbf{0}$ in the properly supported structure, and the equivalent pseudo load can be found from Eq. 2a by solving the following linear system:

$$\left(\boldsymbol{\mathcal{B}}^{\mathrm{ap}}\mathbf{p}^0\right)(t) = -\mathbf{a}^{\mathrm{L}}(t). \tag{3}$$

Equation 3 is a linear system of Volterra integral equations that should be discretized and solved numerically. Here, the solution is symbolically denoted by

$$\mathbf{p}^0(t) = -\left([\boldsymbol{\mathcal{B}}^{\mathrm{ap}}]^+ \, \mathbf{a}^{\mathrm{L}}\right)(t), \tag{4}$$

where the superscript $+$ denotes the (regularized) inverse operator. Computed the pseudo load, Eq. 2b can be used to compute the modeled measurements in the virtually supported structure: upon substitution of $\mathbf{p}^0(t)$ into Eq. 2b, the following formula is obtained:

$$\mathbf{u}(t) = \mathbf{u}^{\mathrm{L}}(t) - \left(\boldsymbol{\mathcal{B}}^{\mathrm{up}} [\boldsymbol{\mathcal{B}}^{\mathrm{ap}}]^+ \, \mathbf{a}^{\mathrm{L}}\right)(t). \tag{5}$$

2.3 Non-impulsive constraining excitations

The response of the virtually supported structure Eq. 5 is based on the assumption that the constraining excitations are impulsive. In practice, such excitations might be hard to apply, but this assumption can be relaxed, so that the experimentally applied constraining excitations can be non-impulsive, if assumed that the pseudo loads are expressed in the form of the convolution

$$p_i^0(t) = (q_i * p_i)(t) = \int_0^t q_i(t-\tau)p_i(\tau)\,\mathrm{d}\tau, \tag{6}$$

in which $q_i(t)$ denote the actually applied non-impulsive constraining excitations. This equation, collected for all i, takes in the operator notation the form of

$$\mathbf{p}^0(t) = (\boldsymbol{\mathcal{Q}}\mathbf{p})(t), \tag{7}$$

which makes use of the corresponding diagonal matrix convolution operator $\boldsymbol{\mathcal{Q}}$. As a result, Equations 2 take the following form:

$$\mathbf{a}(t) = \mathbf{a}^{\mathrm{L}}(t) + (\boldsymbol{\mathcal{B}}^{\mathrm{ap}}\mathbf{p})(t), \tag{8a}$$

$$\mathbf{u}(t) = \mathbf{u}^{\mathrm{L}}(t) + (\boldsymbol{\mathcal{B}}^{\mathrm{up}}\mathbf{p})(t), \tag{8b}$$

where, in comparison to Eqs. 2, the following substitutions have been performed:

$$\mathcal{B}^{\mathrm{ap}} \leftarrow \mathcal{B}^{\mathrm{ap}}\mathcal{Q}, \qquad\qquad\qquad \mathcal{B}^{\mathrm{up}} \leftarrow \mathcal{B}^{\mathrm{up}}\mathcal{Q}. \qquad (9)$$

In both cases $\mathcal{B}^{\mathrm{ap}}$ and $\mathcal{B}^{\mathrm{up}}$ are the matrix convolution operators with the measured responses of the constraining and basic sensors to the constraining excitations. Equations 8 yield

$$\mathbf{u}(t) = \mathbf{u}^{\mathrm{L}}(t) - \left(\mathcal{B}^{\mathrm{up}} \left[\mathcal{B}^{\mathrm{ap}}\right]^{+} \mathbf{a}^{\mathrm{L}} \right)(t), \qquad (10)$$

which is formally the same as Eq. 5. The operator $\mathcal{Q}$ does not appear explicitly in Eqs. 8 and 10, hence the constraining excitations $q_i(t)$ need not be measured. However, they affect the properties of the operator $\mathcal{B}^{\mathrm{ap}}$ and thus the accuracy of the result. In practice, quasi-impulsive excitations, obtained e.g. with modal hammer, tend to provide good results.

2.4 Computations in frequency domain

Thus far all the derivations are performed in time domain. Equations 8 are large Volterra integral equations, and Eq. 10 involves computing a solution to a system of such equations. In time domain, this can be a computationally demanding task, as it involves computing a solution to a very large and ill-conditioned linear system, which has the dimensions proportional to the number of the considered time steps. As a result, the manageable length of the measurement time interval is significantly limited. However, the problem can be formulated and solved in frequency domain, which dramatically improves the computational efficiency.

The derivations can be repeated in frequency domain in an analogous way. The naming convention is the same as in Table 1, with the exception that the responses are complex amplitudes that depend on the frequency ω. The frequency-domain counterparts of Eqs. 2 are

$$\mathbf{a}(\omega) = \mathbf{a}^{\mathrm{L}}(\omega) + \mathbf{B}^{\mathrm{ap}}(\omega)\mathbf{p}^{0}(\omega), \qquad (11a)$$

$$\mathbf{u}(\omega) = \mathbf{u}^{\mathrm{L}}(\omega) + \mathbf{B}^{\mathrm{up}}(\omega)\mathbf{p}^{0}(\omega), \qquad (11b)$$

where $\mathbf{p}^{0}(\omega)$ is the frequency-domain pseudo load that models the support reaction forces and $\mathbf{B}^{\mathrm{ap}}(\omega)$ and $\mathbf{B}^{\mathrm{ap}}(\omega)$ are complex matrices. In contrast to Eqs. 2, which constitute a large single system of Volterra integral equations, Equations 11 yield for each ω a different linear system. Thus, the following frequency-domain counterpart of Eq. 3,

$$\mathbf{B}^{\mathrm{ap}}(\omega)\mathbf{p}^{0}(\omega) = -\mathbf{a}^{\mathrm{L}}(\omega), \qquad (12)$$

is a matrix equation of a moderate size: the number of unknowns equals the number of the to-be-supported DOFs (constraining sensors). It needs to be solved separately for each ω of interest. Finally, in frequency domain Eq. 10 assumes the following form:

$$\mathbf{u}(\omega) = \mathbf{u}^{\mathrm{L}}(\omega) - \mathbf{B}^{\mathrm{up}}(\omega) \left[\mathbf{B}^{\mathrm{ap}}(\omega)\right]^{+} \mathbf{a}^{\mathrm{L}}(\omega), \qquad (13)$$

where $- \left[\mathbf{B}^{\mathrm{ap}}(\omega)\right]^{+} \mathbf{a}^{\mathrm{L}}(\omega)$ denotes the solution to Eq. 12. In practice, even repeated solutions of Eq. 12 are considerably faster than a single solution of the integral equation Eq. 3. The process is even less time-consuming, if only a limited number of frequencies ω is of interest instead of the full spectrum.

3. SUBSTRUCTURE ISOLATION AND LOCAL ANALYSIS

A series of virtual supports placed in all interface DOFs of the considered substructure can be used to eliminate all influences of the global structure from the measured basic response of the substructure. Such an approach can be used for complete virtual *substructure isolation*. However, a straightforward application of the virtual supports would be faced with the four following difficulties that can significantly limit the potential for practical applications: (1) the global structure needs to be linear, (2) constraining excitations need to be placed in all DOFs of the interface, (3) virtual fixed supports need displacement sensors in all interface DOFs, (4) zero initial conditions are required (no online applications). All these requirements can be considerably relaxed or dropped, so that

1. Only the substructure is required to be linear, while the global structure besides the substructure can be nonlinear, yielding, changing or simply unknown.

2. Constraining excitations can be placed in the DOFs of the interface or anywhere in the outside structure (but not in the DOFs internal to the substructure). In online applications, operational loads can be used for this purpose.

3. In addition to fixed boundary conditions modeled with virtual fixed supports, virtual free supports can be introduced to model free boundary conditions. Virtual free supports require strain measurements instead of displacements (velocities or accelerations), which can be more feasible, especially in rotational DOFs of frame structures. Virtual fixed and free supports can be simultaneously used in different DOFs of a single node in order to model nodal virtual supports of various types, such as virtual pinned supports.

4. Non-zero initial conditions are possible at the cost of an additional linear trend and a free response component that may occur in the computed response, see Section 3.5

3.1 Naming convention

The same convention is used as in the case of virtual supports. The excitations are divided into: (1) *Constraining excitations*, which are applied in the DOFs of the interface or in the DOFs of the outside structure. The number of constraining excitations must not be smaller than the number of the interface DOFs. They need not be impulsive, and each of them results in a vector $\mathbf{q}_i^{\mathrm{I}}(t)$ of the generalized interface forces that excites the substructure. (2) *Basic excitation*, which is the external excitation $\mathbf{f}(t)$ placed inside the substructure. The constraining excitations can be placed also outside the interface, that is not necessarily only in the to-be-supported DOFs of the interface. It is possible, because the response of the outside structure can be disregarded, while the substructural response to the ith constraining excitation is exactly the same as the response of the substructure to $\mathbf{q}_i^{\mathrm{I}}(t)$.

The responses are measured by the two following types of sensors: (1) *Constraining sensors*, which are linear sensors (displacement, velocity or acceleration) that implement the virtual

supports and need to be placed in all DOFs of the interface. (2) *Basic sensors*, which are placed inside the substructure. The purpose of isolation is to compute the response to the basic excitation that would be measured by the basic sensors, if the substructure was physically isolated from the rest of the global structure. As before, there are a total of four different types of the measured responses, which are named as in Table 1.

3.2 Isolation in time domain

The substructure is virtually isolated by placing virtual fixed supports in all DOFs of its interface with the global structure. The supports are modeled by the pseudo load vector $\mathbf{p}^0(t)$ that would equal the generalized support reaction forces, if the substructure was physically supported. As in Eq. 6, the pseudo load vector is represented as

$$\mathbf{p}^0(t) = \sum_i \int_0^t \mathbf{q}_i^{\mathrm{I}}(t-\tau) p_i(\tau) \, \mathrm{d}\tau, \tag{14}$$

where i indexes constraining excitations, $p_i(t)$ are certain unknown functions, and $\mathbf{q}_i^{\mathrm{I}}(t)$ are the generalized interface forces that correspond to the ith constraining excitation $q_i(t)$. Equation 14 can be stated in the operator notation as

$$\mathbf{p}^0 = \boldsymbol{\mathcal{Q}}^{\mathrm{I}} \mathbf{p}, \tag{15}$$

where $\boldsymbol{\mathcal{Q}}^{\mathrm{I}}$ is the matrix convolution operator that, unlike $\boldsymbol{\mathcal{Q}}$ in Eq. 7, is not diagonal.

The considered substructure is assumed to be linear. For the substructure, the constraining excitations and the corresponding interface excitations $\mathbf{q}_i^{\mathrm{I}}(t)$ are equivalent. Thus, the responses of the basic and constraining sensors in a supported substructure can be modeled as follows:

$$\mathbf{a}(t) = \mathbf{a}^{\mathrm{L}}(t) + \left(\boldsymbol{\mathcal{B}}^{\mathrm{ap}} \mathbf{p}\right)(t), \tag{16a}$$

$$\mathbf{u}(t) = \mathbf{u}^{\mathrm{L}}(t) + \left(\boldsymbol{\mathcal{B}}^{\mathrm{up}} \mathbf{p}\right)(t), \tag{16b}$$

where $\boldsymbol{\mathcal{B}}^{\mathrm{ap}}$ and $\boldsymbol{\mathcal{B}}^{\mathrm{up}}$ are matrix convolution operators with the measured responses to the constraining excitations of the constraining and basic sensors respectively. The interface responses $\mathbf{a}(t)$ vanish in a properly isolated substructure, $\mathbf{a}(t) = \mathbf{0}$, and Eq. 16a yields

$$\left(\boldsymbol{\mathcal{B}}^{\mathrm{ap}} \mathbf{p}\right)(t) = -\mathbf{a}^{\mathrm{L}}(t). \tag{17}$$

Equations 16b and 17 yield together the formula

$$\mathbf{u}(t) = \mathbf{u}^{\mathrm{L}}(t) - \left(\boldsymbol{\mathcal{B}}^{\mathrm{up}} \left[\boldsymbol{\mathcal{B}}^{\mathrm{ap}}\right]^+ \mathbf{a}^{\mathrm{L}}\right)(t), \tag{18}$$

which is formally the same as Eqs. 5 and 10. The operator $\boldsymbol{\mathcal{Q}}^{\mathrm{I}}$ does not appear in Eqs. 16 nor in Eq. 18, hence neither the constraining excitations $q_i(t)$ nor the equivalent interface excitations $\mathbf{q}_i^{\mathrm{I}}(t)$ need to be known. However, the character and placement of the constraining excitations affect the properties of the operator $\boldsymbol{\mathcal{B}}^{\mathrm{ap}}$, which is inverted in Eq. 18, and thus the accuracy of the isolation, see Section 4.1
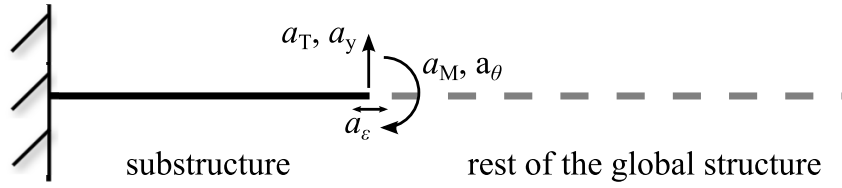
Figure 1. A substructure of a 2D beam (axial displacements of the interface ignored)
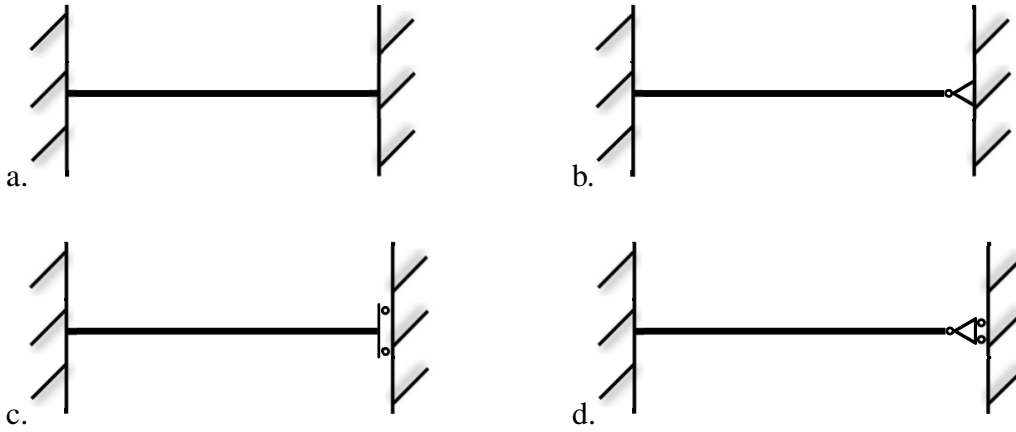
Figure 2. The four types of nodal virtual supports defined in Eqs. 19

3.3 Isolation with other types of virtual supports

Up to now, the constraining sensors have been assumed to measure displacement, velocity or acceleration, so that they implement fixed boundary conditions. Other kinds of virtual supports can be also used to emulate other types of boundary conditions and nodal virtual supports. In the following, isolation of a 2D beam is used as an example. Figure 1 shows the structure, the substructure to be isolated and the physical quantities of interest at the interface: the internal shear force $a_T(t)$, the internal bending moment $a_M(t)$, the vertical displacement $a_y(t)$, the rotation $a_\theta(t)$ and the strain $a_\varepsilon(t)$. For the moment, the axial displacement and axial force are ignored for the sake of simplicity: in their absence, the strain $a_\varepsilon(t)$ (measured off the neutral axis) is proportional to the bending moment $a_M(t)$, but much easier to measure. The mentioned quantities can be used to formulate four different types of boundary conditions,

$$
\text{a.} \begin{cases} 0 = a_y(t), \\ 0 = a_\theta(t), \end{cases} \quad \text{b.} \begin{cases} 0 = a_y(t), \\ 0 = a_\varepsilon(t), \end{cases} \quad \text{c.} \begin{cases} 0 = a_T(t), \\ 0 = a_\theta(t), \end{cases} \quad \text{d.} \begin{cases} 0 = a_T(t), \\ 0 = a_\varepsilon(t), \end{cases} \quad (19)
$$

where the strain is used as a substitute for the internal bending moment. Equations 19 define four kinds of nodal virtual supports that can be applied to isolate the substructure, see Figure 2.

If axial displacement and axial force are to be considered, the strain is no longer a direct substitute for the internal bending moment. In such a case, two strain sensors can be placed on the opposite faces of the beam in the same distance from its neutral axis: the axial stress and the bending moment will be proportional to the sum and to the difference of their measurements.

3.4 Isolation in frequency domain

A frequency-domain formulation is proposed to decrease the computational effort. The frequency-domain counterparts of Eqs. 16 have the form of the following matrix equations:

$$\mathbf{a}(\omega) = \mathbf{a}^{\mathrm{L}}(\omega) + \mathbf{B}^{\mathrm{ap}}(\omega)\mathbf{p}(\omega), \tag{20a}$$

$$\mathbf{u}(\omega) = \mathbf{u}^{\mathrm{L}}(\omega) + \mathbf{B}^{\mathrm{up}}(\omega)\mathbf{p}(\omega). \tag{20b}$$

In a properly isolated substructure, the response of the interface sensors vanish, $\mathbf{a}(\omega) = \mathbf{0}$, thus

$$\mathbf{B}^{\mathrm{ap}}(\omega)\mathbf{p}(\omega) = -\mathbf{a}^{\mathrm{L}}(\omega), \tag{21}$$

$$\mathbf{u}(\omega) = \mathbf{u}^{\mathrm{L}}(\omega) - \mathbf{B}^{\mathrm{up}}(\omega)\left[\mathbf{B}^{\mathrm{ap}}(\omega)\right]^{+}\mathbf{a}^{\mathrm{L}}(\omega). \tag{22}$$

Equations 21 and 22 are frequency-domain counterparts of the time-domain Eqs. 17 and 18. The most important differences between the two formulations can be summarized as follows:

1. Equation 21 is a separate matrix equation for each frequency line ω, and so it might be solved only a limited number of times. The time-domain Eq. 17 is a single system of Volterra integral equations that needs to be solved once and for all.

2. Equation 21 is of a significantly smaller size than the discretized version of Eq. 17. The former system has the dimensions of *number of interface sensors* $\times$ *number of constraining excitations*, while in the latter system both dimensions are N_{t} times larger.

3. The time-domain system is extremely ill-conditioned. The frequency-domain system is well-conditioned for most of ω, provided the constraining excitations are properly placed.

4. The time-domain system is constructed using directly measured discrete time-domain responses, while the frequency-domain system needs an initial pre-processing of the measurement data (windowing, averaging, discrete Fourier transform, etc.).

3.5 Online isolation

Above, zero initial conditions are assumed, which excludes online isolation in structures under operational loads. Still, online isolation is possible, and the assumption of zero initial conditions can be dropped. It affect the computed response of the isolated substructure:

- The nonzero initial conditions of the DOFs internal to the substructure result in a free response component in the computed response of the isolated substructure.

- The nonzero initial conditions of the interface DOFs can result in an artificial constant bias or a linear trend appearing in the computed response of the isolated substructure. For example, if accelerometers are used on the interface and strain sensors inside the substructure, a linear trend can occur; with a velocity sensor on the interface, a constant bias can appear in the computed internal strain response, etc. Such a response can be still used with many typical SHM methods, such as those based on the local natural frequencies, as they can be directly extracted from the computed response.

4. APPLICATION OF THE METHOD

4.1 Excitations

The constraining excitations can be of any type, but their character and placement influence the conditioning of Eq. 18, and thus the computed response. They should provide full dynamic information about the interface. The following hints can be considered:

1. In order to ensure a high signal-to-noise ratio, the constraining excitations should be placed near the interface rather than far away from it.

2. The constraining excitations should be applied in different points and in various directions. In this way, there are more chances that the constraining responses are independent.

3. The constraining excitations should not be very soft or too hard. A soft excitation may excite only low frequencies, while a hard excitation may result in only high-frequency response. In both cases, information in a certain frequency range would be lost.

4.2 Identification at the substructural level

Equations 18 and 22 yield the response of the isolated substructure to the basic excitation. The isolated substructure has the same physical parameters as the actual substructure, but constitutes a (virtual) system that is independent from the outside structure and which has its own characteristics that can be found by investigation of the constructed response and the basic excitation. Local damage identification can be then performed by any of the standard methods that have been originally aimed at global identification. In the experimental examples below, the substructure is identified by updating selected parameters of its local FE model.

In time-domain applications, local damage of the substructure is identified via a comparison of the discrete response $\mathbf{u}$ of the isolated substructure with the response $\mathbf{u}^{\mathrm{FE}}(\boldsymbol{\mu})$ that is computed using its FE model and which depends on the vector $\boldsymbol{\mu}$ of unknown structural parameters. The vector $\boldsymbol{\mu}$ is treated as an optimization variable, and the damage is identified by minimizing

$$F(\boldsymbol{\mu}) := \frac{\|\mathbf{u} - \mathbf{u}^{\mathrm{FE}}(\boldsymbol{\mu})\|^2}{\|\mathbf{u}\|^2}. \tag{23}$$

In frequency-domain application, if the basic excitation is a short quasi-impulsive load, then the constructed response is a free response of the isolated substructure. Its local natural frequencies ω_i and mode shapes ϕ_i can be identified e.g. by the Eigensystem Realization Algorithm (ERA). A local damage is then identified by minimizing the following discrepancy between the identified modes with the modes computed using a local FE model:

$$F(\boldsymbol{\mu}) := \sum_i \left| \frac{\omega_i - \omega_i^{\mathrm{FE}}(\boldsymbol{\mu})}{\omega_i} \right|^2 + \kappa \sum_i \left| 1 - \mathrm{MAC}\left(\phi_i, \phi_i^{\mathrm{FE}}(\boldsymbol{\mu})\right) \right|^2, \tag{24}$$

where $\omega_i^{\mathrm{FE}}(\boldsymbol{\mu})$ and $\phi_i^{\mathrm{FE}}(\boldsymbol{\mu})$ are respectively the ith natural frequency and mode shape of the numerical model of the isolated substructure, and κ is a weighting factor of the mode shape errors that are computed using the Modal Assurance Criterion (MAC).
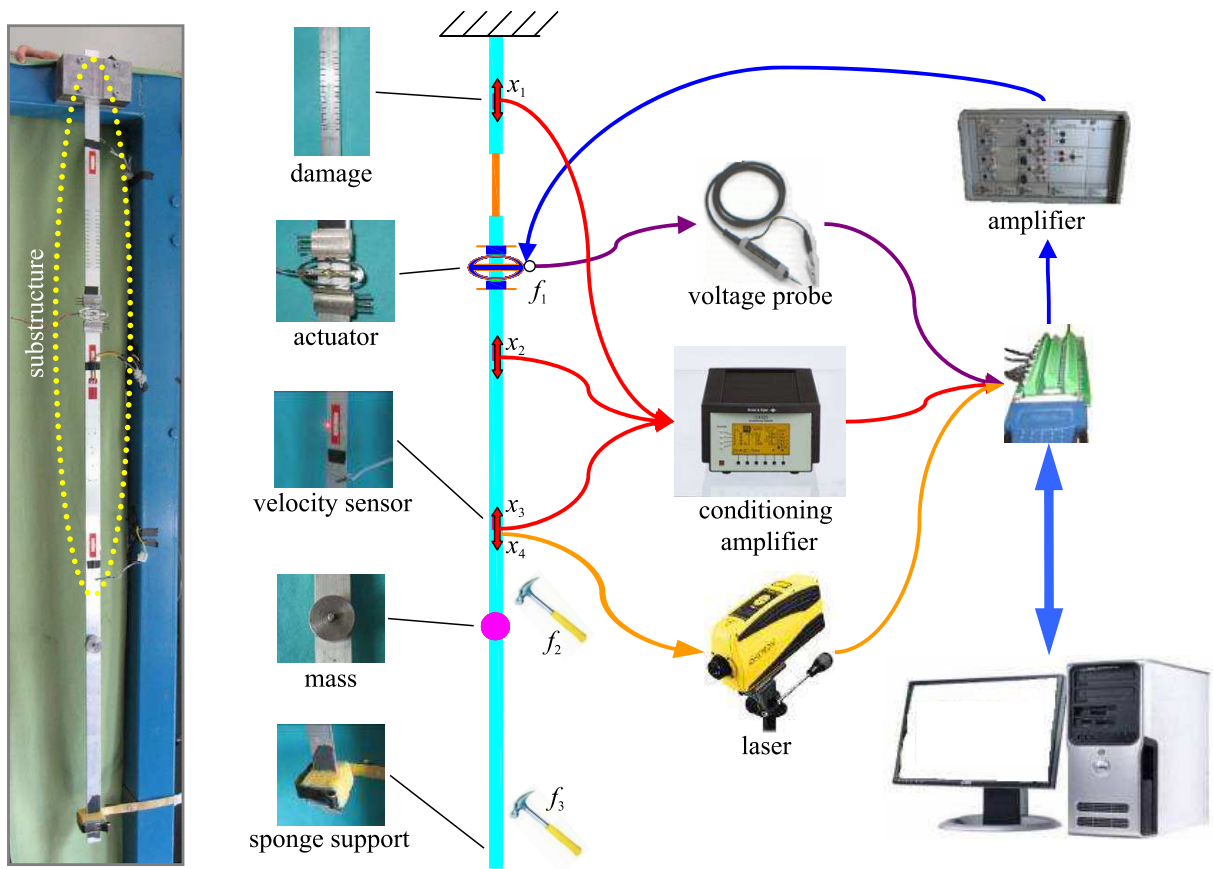
Figure 3. The setup

5. EXPERIMENTAL EXAMPLE

In the experimental example, time-domain and frequency-domain isolation is used to construct the time-domain responses of the isolated substructure to a windowed sine pulse or to a modal hammer excitation, respectively. Then a local damage is identified by Eqs. 23 and 24. Two modifications of the global structure are used to test the robustness of the isolation with respect to unknown modifications of the outside structure.

5.1 Experimental setup

The specimen, an aluminum cantilever beam, see Figure 3, has the length of 136.15 cm and a cross-section of 2.7 cm × 0.31 cm. The fixed end is clamped to a stable frame. Young's modulus is 70 GPa, and the density is 2700 kg/m^3. Its upper part (of length 79.4 cm) is the substructure to be identified. It is damaged by cutting even notches near the fixed end on the length of 10.2 cm, which decreases the stiffness of the damaged segment to 42% of its original stiffness and leaves the mass nearly unchanged, see Figure 4 (left). Three different global structures that share the same substructure are used to verify the robustness of the isolation with
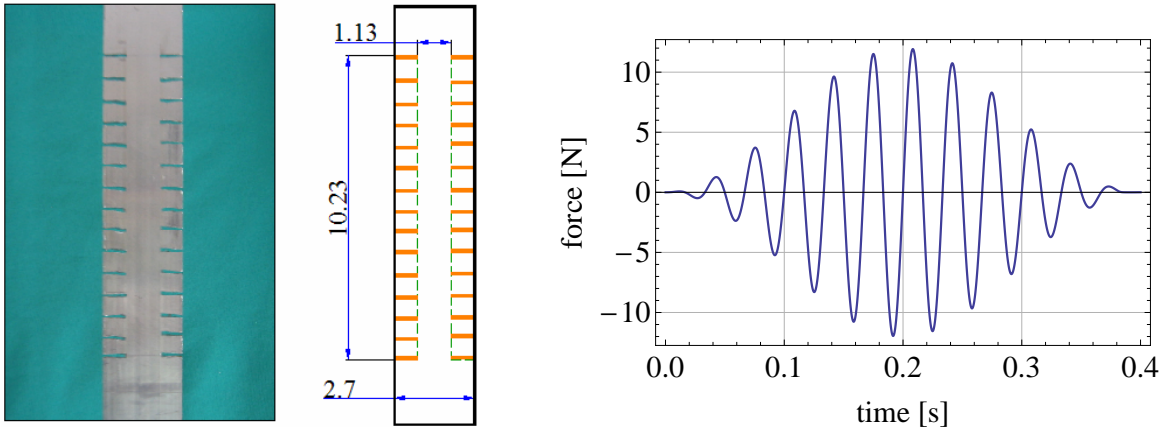
Figure 4. (left) The to-be-identified damage of a section of the beam (stiffness decreased to 42%, mass unchanged); (right) The basic excitation f_1 for time-domain identification: a windowed sine pulse $\sin 60\pi t$ applied using the piezo-actuator (APA)

Table 2. The three global structures with the same substructure

symbol	outside structure
b_1	original beam
b_2	original beam with an additional unknown mass
b_3	original beam with a "sponge support"

respect to unknown modifications of the outside structure. Based on the same beam, the outside structure is modified by fixing an unknown additional mass or by mounting a "sponge support" in place of the free end, see Table 2. Two kinds of the basic excitation are separately applied to be used with different isolation methods:

1. For time-domain isolation, a windowed sine pulse $\sin(60\pi t)$ is applied using an Amplified Piezo Actuator (APA), see Figure 4 (right). The APA is fixed to the inner substructure in such a way that it can be assumed to apply a pure moment load.

2. For frequency-domain isolation, the APA is not mounted and an impact by a simple uninstrumented hammer is used instead in the role of the basic excitation.

Three piezoelectric patches are glued to the beam to measure the strain x_1, x_2 and x_3, and the transverse interface velocity x_4 is measured using a laser vibrometer, see Figure 3. Raw voltage readings are used in computations in order to avoid unnecessary scaling of the measurement noise. To reduce the measurement noise, each excitation is repeated 4 to 5 times and the averaged responses are used for identification. The sampling frequency is 10 kHz. The sampling time is 0.4 s (4000 time steps) for the time-domain isolation and 4 s (40000 time steps) for the frequency-domain isolation.
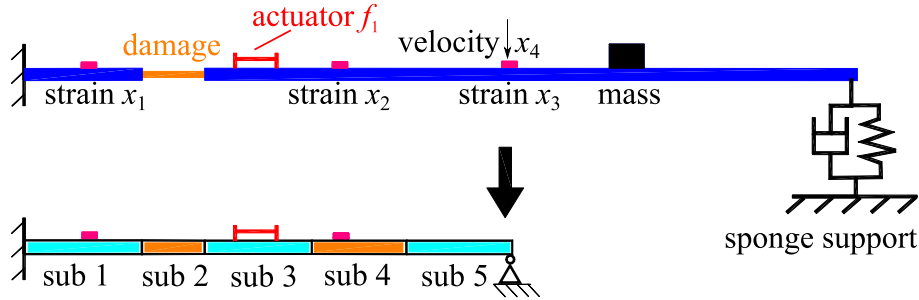
Figure 5. Substructure isolation with a single virtual pinned support in the interface node (free support in the rotational DOF, fixed support in the transverse DOF, negligible axial distortions)

A single virtual pinned support is used to isolate the substructure in the interface node, see Figure 5. As axial distortions are negligible, it is implemented by the two interface sensors: the strain sensor x_3 plays the role of the free support in the rotational DOF and constrains the bending moment, while the velocity sensor x_4 plays the role of the fixed support and constrains the transverse displacement. The two other strain sensors (x_1 and x_2) are placed in the inner substructure and used for damage identification.

Two virtual supports are used, and two constraining excitations are thus required. They are applied at two points of the outside structure and denoted by f_2 and f_3, see Figure 3. A simple uninstrumented hammer is used to apply simple transverse impacts. In order to ensure that the corresponding responses are independent, f_2 and f_3 are placed far from each other.

The substructure is divided into five segments, see Figure 5. The damage is modeled by decreasing the stiffnesses of the segments and represented by the vector of their stiffness reduction ratios $\boldsymbol{\mu} = \{\mu_1, \mu_2, \ldots, \mu_5\}$. In experiment, only the second segment is actually damaged,

$$\boldsymbol{\mu}_{\text{actual}} := [1.00, 0.42, 1.00, 1.00, 1.00]^{\text{T}}. \tag{25}$$

An updated FE model of the undamaged isolated substructure is available. The three global structures are not modeled parametrically.

5.2 Isolation and identification in time domain

The APA is used to apply the basic excitation f_1 depicted in Figure 4 (right). First, the responses of the four sensors x_1 to x_4 are measured in three global structures b_1 to b_3. Then, the responses to the constraining excitations f_2 and f_3 are measured. Finally, the substructure is isolated by Eq. 18. The process involves the responses to the basic and constraining excitations, which can be measured in any of the three global structures b_1, b_2 or b_3. Figure 6 (top left) compares the constructed responses x_1 and x_2 of the isolated substructure to the responses of the undamaged substructure as simulated using its FE model. The constructed responses are visually indistinguishable, which is consistent with the fact that all three global structures share the same substructure. The influences of its outside, including the additional mass and the sponge support, are eliminated. The difference between the constructed and the simulated
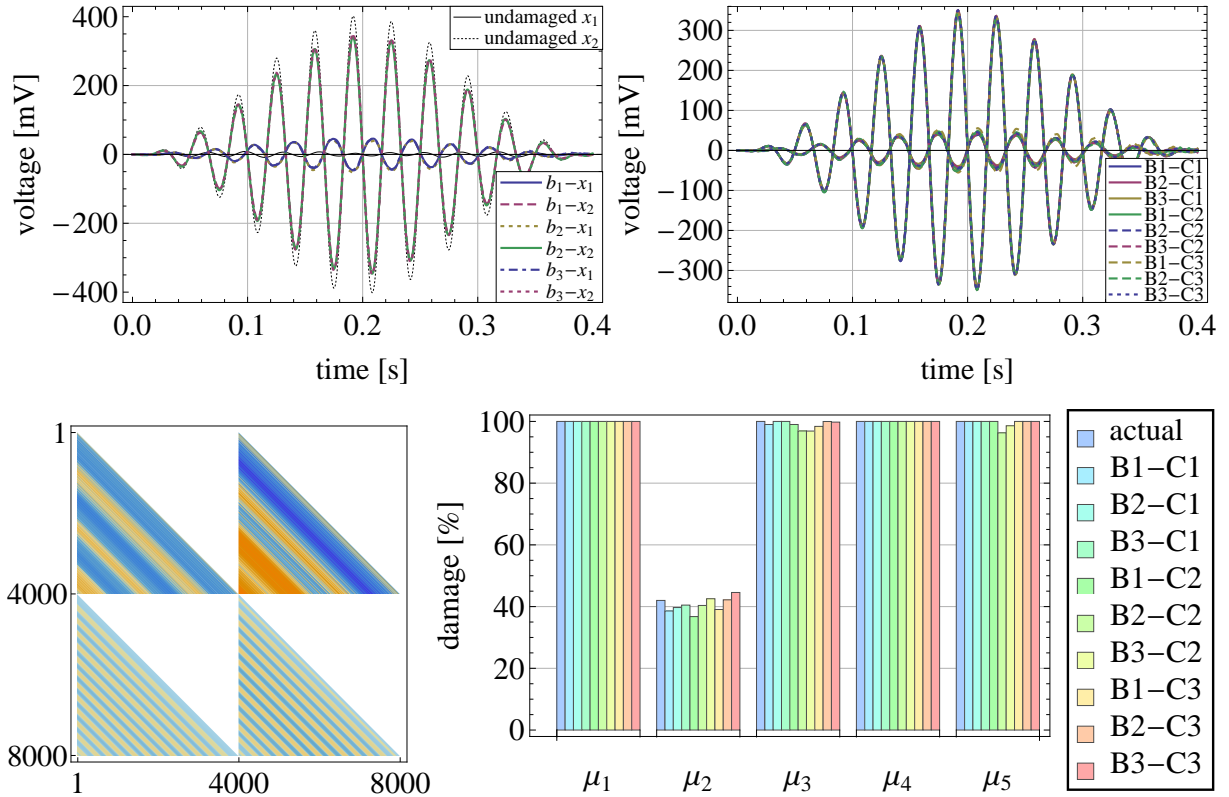
Figure 6. Isolation in time domain. (top left) Constructed responses x_1 and x_2 of the same substructure isolated out of the three considered global structures b_1, b_2 and b_3 compared to the FEM-based responses of the undamaged substructure; (top right) The nine constructed responses of the isolated substructure; (bottom left) Block Toeplitz structure of the matrix $\mathbf{B}^{\mathrm{ap}}$ in structure b_1; (bottom right) Actual and identified damage

responses is related to the local damage and can be exploited for its identification. In order to verify the robustness of the isolation method in a case of a global structure that changes during the measurements, the responses to the basic and constraining excitations can be measured in different global structures. There are three structures and nine possible combinations denoted by "Bi–Cj" (basic excitation in b_i, constraining excitation in b_j). Figure 6 (top right) plots the nine responses constructed this way. They match well, which confirms that the constructed response is not influenced by developing outside modifications, provided the substructure remains the same. Figure 6 (bottom left) illustrates the block Toeplitz structure of the matrix $\mathbf{B}^{\mathrm{ap}}$.

Damage identification in time domain amounts to the minimization of the objective function Eq. 23 with respect to the five stiffness reduction ratios μ_1 to μ_5, subject to $0 < \mu_i \leq 1$ for $i = 1, \ldots, 5$. The identification results are shown in Figure 6 (bottom right) and compared to the actual values. Both the location and the extent of the damage are identified with a high accuracy. The damage is identified at the substructural level, that is no FE model of the global structure is used for this purpose.
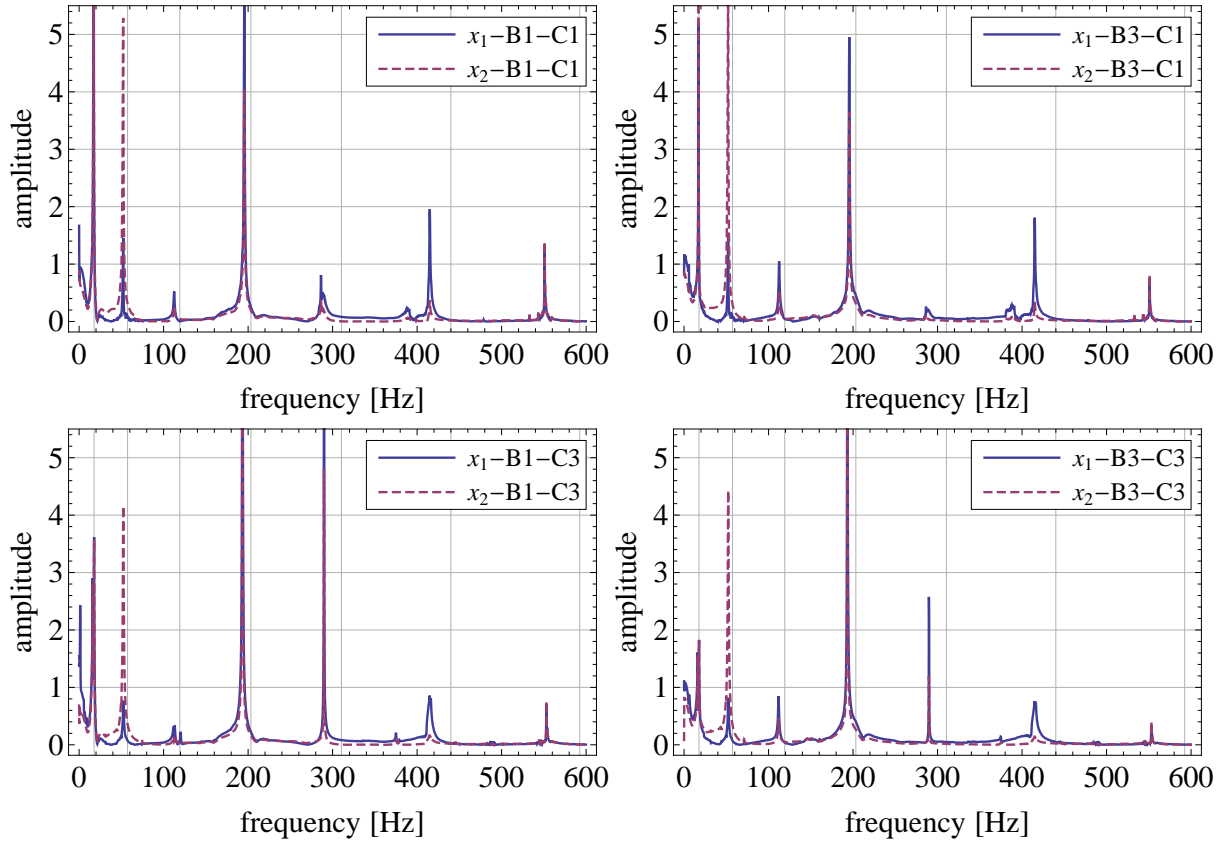
Figure 7. Isolation in frequency domain. Spectra of the four constructed responses to f_1: (top left) B1–C1; (top right) B3–C1; (bottom left) B1–C3; (bottom right) B3–C3. The vertical gridlines mark the natural frequencies of the undamaged isolated substructure

5.3 Isolation and identification in frequency domain

For isolation in frequency domain, the beams b_1 and b_3 are used without the APA. Instead, the basic excitation by a simple uninstrumented hammer at the same location is used. The responses of four sensors are measured in the two global structures. The identification is based on fitting the natural frequencies, and hence a long time interval of 4 s (40 000 time steps) is used.

The responses to basic and constraining excitations used in the isolation formula Eq. 22 can be measured in different global structures. Two structures are used, and there are four combinations. The spectra of the constructed responses x_1 and x_2 are shown in Figure 7. The vertical gridlines mark the natural frequencies computed using the FE model of the undamaged structure. They are clearly different than the plot peaks; the differences are due to the damage. The first seven natural frequencies are obtained by peak-picking (besides the seven pronounced peaks there are two small spurious peaks at approx. 2 Hz and 375 Hz. They correspond to the first natural frequency of the global structure and to its first torsional mode. The former is not

Table 3. Isolation in frequency domain. Natural frequencies of the isolated substructure in Hz

no.	theoretical FEM		identified experimentally			
	intact	damaged	B1–C1	B3–C1	B1–C3	B3–C3
1	17.64	17.47	17.08	17.08	17.69	17.70
2	57.33	52.00	52.14	52.14	52.27	52.27
3	119.15	112.94	112.49	112.52	113.25	111.83
4	203.28	195.65	195.48	195.51	193.27	193.27
5	310.44	290.01	286.27	286.31	289.84	289.84
6	439.89	413.88	414.96	414.97	414.81	414.82
7	592.37	550.98	550.99	550.99	553.04	553.04
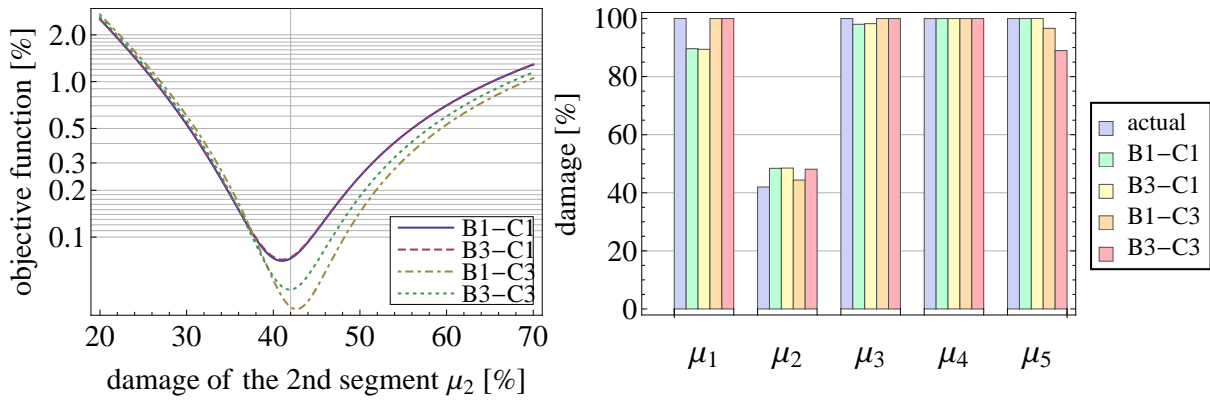
Figure 8. Isolation in frequency domain: (left) Objective functions in the four considered cases. Only μ_2 is assumed to be unknown. The vertical gridline mark the actual damage of 42%; (right) Actual damage and the results of full identification

fully isolated, while the latter cannot be modeled using a plane beam model employed here), see Table 3. They are in good agreement with the natural frequencies computed using local FE model and the actual damage extents. The identified natural frequencies are almost the same in all four combination cases.

Damage identification is based on updating the local FE model of the substructure to fit its first seven natural frequencies to the frequencies listed in Table 3. The first summand in Eq. 24 is used as the objective function. First, it is assumed that the location of the damage is known, so that only μ_2 is unknown; Figure 8 (left) plots the four objective functions in dependence on μ_2. All the four minima are located close to the actual value of 42%, which is marked with the vertical gridline. Then, the full identifications are performed with respect to all five stiffness reduction ratios. The results are shown in Figure 8 (right). Identification accuracy, even if slightly lower than in the time-domain analysis, is still very good in terms of localization as well as quantification of the damage.

Jilin Hou, Łukasz Jankowski and Jinping Ou.

6. ACKNOWLEDGEMENTS

References

[1] C. Koh and K. Shankar. Substructural identification method without interface measurement. *Journal of Engineering Mechanics (ASCE)* 129, 769–776, 2003.

[2] C. Koh, L. See and T. Balendra. Estimation of structural parameters in time domain: a substructure approach. *Earthquake Eng. and Struct. Dynamics* 20, 787–801, 1991.

[3] C. Koh, B. Hong and C. Liaw. Substructural and progressive structural identification methods. *Engineering Structures* 25, 1551–1563, 2003.

[4] C.-B. Yun and H.-J. Lee. Substructural identification for damage estimation of structures. *Structural Safety* 19, 121–140, 1997.

[5] K. Tee, C. Koh and S. Quek. Substructural first- and second-order model identification for structural damage assessment. *Earthquake Engineering and Structural Dynamics* 34, 1755–1775, 2005.

[6] K. Tee, C. Koh and S. Quek. Numerical and experimental studies of a substructural identification strategy. *Structural Health Monitoring* 8, 397–410, 2009.

[7] J. Yang and H. Huang. Substructure damage identification using damage tracking technique. *Proc. SPIE 6529*, 2007, 65292R.

[8] Y. Lei, Y. Wu and T. Li. Identification of non-linear structural parameters under limited input and output measurements. *Int. J. of Non-Linear Mechanics* 47, 1141–1146, 2012.

[9] T. Trinh and C. Koh. An improved substructural identification strategy for large structural systems. *Structural Control and Health Monitoring* 19, 686–700, 2012.

[10] Z. Xing and A. Mita. A substructure approach to local damage detection of shear structure. *Structural Control and Health Monitoring* 19, 309–318, 2012.

[11] X. Wang, C. Koh and Z. Zhang. Damage identification based on strain and translational measurements with substructure approach. *Proceedings of the 1st Middle East Conf. on Smart Monitoring, Assessment and Rehabilitation of Civil Structure*, Dubai, 2011.

[12] J. Hou, Ł. Jankowski and J. Ou. Substructural damage identification using Local Primary Frequency. *Proc. of the 11th Int'l Symp. on Struct. Eng. (ISSE 11th)*, Guangzhou, 2010.

[13] J. Hou, Ł. Jankowski and J. Ou. Substructural damage identification using time series of local measured response. *Proc. of the 5th World Conf. on Structural Control and Monitoring (5WCSCM 2010)*, Tokyo, 2010.

[14] J. Hou, Ł. Jankowski and J. Ou. Substructure isolation and identification using FFT of measured local responses. *Proc. of the 5th European Workshop on Structural Health Monitoring (EWSHM 2010)*, Sorrento, 913–918, 2010.

[15] J. Hou, Ł. Jankowski and J. Ou. A substructure isolation method for local structural health monitoring. *Structural Control & Health Monitoring* 18, 601–618, 2011.

[16] J. Hou, Ł. Jankowski and J. Ou. Large substructure identification using substructure isolation method. *Proc. SPIE 8345*, 2012, 83453V.

[17] J. Hou, Ł. Jankowski and J. Ou. Substructure Isolation Method for online local damage identification using time series. *Proc. of the 6th European Workshop on Structural Health Monitoring (EWSHM 2012)*, Dresden, 2012.

[18] J. Hou, Ł. Jankowski and J. Ou. Experimental study of the substructure isolation method for local health monitoring. *Structural Control & Health Monitoring* 19, 491–510, 2012.

[19] K. Dems and Z. Mróz. Identification of damage in beam and plate structures using parameter-dependent frequency changes. *Engineering Computations* 18, 96–120, 2001.

[20] K. Dems and Z. Mróz. Damage identification using modal, static and thermographic analysis with additional control parameters. *Computers and Structures* 88, 1254–1264, 2010.

[21] J. Hou, Ł. Jankowski and J. Ou. Structural damage identification by adding virtual masses. *Structural and Multidisciplinary Optimization*, 2013, doi:10.1007/s00158-012-0879-0

[22] N. Nalitolela, J. Penny and M. Friswell. Updating model parameters by adding an imagined stiffness to the structure. *Mechanical Systems and Signal Processing* 7, 161–172, 1993.

[23] P. Kołakowski, M. Wikło and J. Holnicki-Szulc. The virtual distortion method — a versatile reanalysis tool for structures and systems. *Structural and Multidisciplinary Optimization* 36, 217–234, 2008.